Human Papillomavirus Type 16 L1/L2 VLP Experimental Internalisation by Human Peripheral Blood Leukocytes

Running Title: HPV16 VLP internalisation in human leukocytes.

Aurora Marques Cianciarullo[1,2#], Vivian Szulczewski[1,2], Erica Akemi Kavati[1,2], Tania Matiko Hosoda[1,2], Elizabeth Leão[4], Primavera Borelli[5], Enrique Boccardo[6], Martin Müller[7], Balasubramanyam Karanam[8], and Willy Beçak[1,9]

[1]Laboratory of Genetics, Butantan Institute, Secretary of State for Health, 1500 Dr Vital Brazil Avenue, Sao Paulo, SP 05503-900, Brazil.

[2]Program of Postgraduate Interunits in Biotechnology USP-IBU-IPT, Institute of Biomedical Sciences, University of Sao Paulo, 2415 Prof Lineu Prestes Avenue, Biomedical III Building, University City, Sao Paulo, SP 05508-900, Brazil.

[3]Program of Professional Upgrading at Butantan Institute, Secretary of State for Health, 188 Dr Eneas de Carvalho Aguiar, Sao Paulo, SP 05403-000, Brazil.

[4]ELSME – Dr Elizabeth Leão Specialised Medical Services S/C Ltd., Sao Joaquim Hospital, Real and Meritorious Portuguese Beneficence Association, 694 Martiniano de Carvalho Street, Sao Paulo, SP 01321-000, Brazil.

[5]Laboratory of Experimental and Clinical Haematology, Department of Clinical and Toxicological Analyses, School of Pharmaceutical Sciences, University of Sao Paulo, 580 B17 Prof Lineu Prestes Avenue, University City, Sao Paulo, SP 05508-900, Brazil.

[6]Laboratory of Oncovirology, Department of Microbiology, Institute of Biomedical Sciences, University of Sao Paulo, 1374 Prof Lineu Prestes Avenue, Biomedical II Building, University City, Sao Paulo, SP 05508-900, Brazil.

[7]Tumorvirus-specific Vaccination Strategies, Infection, Inflammation and Cancer Program, German Cancer Research Centre (DKFZ), 242 Im Neuenheimer Feld, Heidelberg 69120, Germany.

[8]Department of Pathology, Johns Hopkins University, Room 38, Cancer Research Building 2, 1550 Orleans Street, Baltimore, MD 21231, USA.

[9]Department of Biology, Federal University of the Latin-America Integration – UNILA, 1842 Silvio Americo Sasdelli Avenue, Vila A, Commercial Lorivo Building, Foz do Iguaçu, PR 85866-000, Brazil.

#Corresponding author: Aurora M. Cianciarullo, Laboratory of Genetics, Butantan Institute, 1500 Dr Vital Brazil Avenue, Sao Paulo, SP 05503-900, Brazil, phone +5511 26279725, fax +5511 26279714, email: aurora.cianciarullo@butantan.gov.br

Footnote: B.K. present addresses Department of Biology and Cancer Research, 1200 W. Montgomery Road, Tuskegee University, Tuskegee, AL 36088, USA.

Keywords: HPV16 L1/L2 VLP, HPV internalisation by lymphocytes, HPV membrane receptors, cancer risk factor, public health.

Grant support: This work was supported by grants from the Foundation for Research Support of the State of Sao Paulo – FAPESP (Process number 2004/15122-5), Butantan Institute and Butantan Foundation, Sao Paulo, SP, Brazil.

Conflicts of interest: The authors disclose no potential conflict of interest with the publication of this article.

Authors email: aurora.cianciarullo@butantan.gov.br, emefjmlisboa@prefeitura.sp.gov.br, erica.kavati@butantan.gov.br, hosodatania@yahoo.com.br, eleao@ibest.com.br, borelli@usp.br, eboccardo@usp.br, martin.mueller@dkfz.de, bkaranam@mytu.tuskegee.edu, wbecak@yahoo.com

ABSTRACT

Human papillomavirus (HPV) accounts for hundreds of thousands of new cases of cervical cancer yearly, and half of these women die of this neoplasia. This study investigates the possibility of HPV16 to infect human peripheral blood leukocytes in *ex vivo* assays. We have developed a leukocyte separation method from heparinized blood samples aiming cellular integrity and viability. We have expressed humanized L1 and L2 viral capsid proteins in HEK293T epithelial human cells, transiently transfecting them with vectors encoding humanized HPVL1 and L2 genes. Recombinant L1/L2 capsid proteins and structured virus-like particles interacted with human peripheral blood mononuclear cells – lymphocytes and monocytes – and were internalised through a pathway involving CD71 transferrin receptors. This was observed, at a percentile of about 54% T-CD4, 47% T-CD8, 48% B-CD20, and 23% for monocytes-CD14. The group of polymorph nuclear cells: neutrophils-eosinophils-basophils group did not internalise any VLPs. Blockage assays with biochemical inhibitors of distinct pathways, like chlorpromazine, rCTB, filipin, nystatin, liquemin, and sodium azide also evidentiated the occurrence of virus-like particles' indiscriminate entrance via membrane receptor on mononuclear cells. This study shows that HPV16 L1/L2 VLPs can interact with the plasma membrane surface and successfully enter lymphocytes without requiring a specific receptor.

IMPORTANCE

Human papillomaviruses (HPVs) belong to the *Papillomaviridae* family and are classified in Alpha papillomavirus, Beta papillomavirus, Gamma papillomavirus, and Mu papillomavirus genera, based on DNA sequence of the L1 gene. They are associated with the development of benignant skin warts, cell transformation and malignant tumours. L1 is

its major capsid protein, and L2 is the minor HPV capsid protein. HPV type 16 is considered a high-risk Alpha papillomavirus due to the association with 50% of cervical cancers worldwide. The most frequent HPV-associated cancer type is cervical cancer, but etiological association has also been demonstrated for carcinomas of the penis, vulva, vagina, anus and oropharynx – including base of the tongue and tonsils – regions. This study indirectly investigates the possibility of HPV16 to infect other cell types *in vitro*, particularly human peripheral blood leukocytes.

INTRODUCTION

In 1974, zur Hausen's researches pointed to the HPV as the major aetiological agent in cervical cancer and, later, its DNA was detected in tumours found in other anogenital regions (1-3). Today, there are more than 200 different types of well characterized HPVs, of which approximately 40 types infect the genital tract. The most frequently found are types 6 and 11 that induce benignant skin warts formation, and types 16 and 18 which are associated to cancer development. There are at least 12 HPV types that according to the Agency for Research on Cancer (IARC) are considered oncogenic to humans (4, Papillomavirus Episteme (PaVE); http://pave.niaid.nih.gov/#home). Among them, HPV16 and HPV18 are those responsible for approximately 70% of all cervical cancers (4, 5). In 2025, the projected global estimate of cervical cancer is expected to rise to 720,415 new cases per year, and it is expected that half of these women will die of this neoplasia (5). However, the difficulty to obtain enough viable wild types or recombinant HPV particles has limited researches to distinct aspects of virus biology (6). All viruses enter host cells to survive, replicate and evade the immune system. So far, the entry of HPV and its traffic through the host cells are still not completely elucidate (7). Several studies describe this

process like a complex set of interactions among different pathways, receptors, co-receptors and co-factors. In keratinocytes, HPV seems to be internalised via clathrin-dependent endocytic mechanisms, but it might use alternative uptake pathways to enter cells, such as a caveolae-dependent route, among others depending on viral type (6-9).

Currently, HPV is recognised as one of the main causes of infection-related cancer worldwide, as well as the causal factor of other diseases. Infection with high-risk HPV types is the aetiological cause of cervical cancer and is strongly associated with a significate fraction of penile, vulvar, vaginal, anal and oropharyngeal cancers (10, 11). HPVs are responsible for approximately 88% of anal cancer and 95% of anal intraepithelial neoplasia grades 2/3 lesions, and 40%-50% of penis and vulvar cancers (10). In oropharyngeal cancers, HPV DNA was detected in 35%-50% cases (10). In all HPV-positive non-cervical cancers, HPV16 is the most common HPV type detected, followed by HPV types 18, 31, 33 and 45. Among the non-cancerous HPV-associated conditions, genital warts and recurrent respiratory papillomatosis are surely linked to HPV6 and 11 (10). In addition, it was demonstrated recently that HPV16 virus-like particles (VLPs) L1/L2 interact with haematopoietic precursor stem cells, present in the amniotic fluid from healthy pregnant women (12). Whereas new pathologies are increasingly being associated to the HPVs; the responsibility and costs of HPV-associated diseases and cancer remain an important public health issue in all countries, regardless of their economic developmental level (13). Due to the continuous worldwide propagation of HPV it is necessary to investigate the possibility of HPV internalisation by different human cell types. In the present study, we addressed the capacity of HPV16 L1/L2 VLP entrance/uptake of – in peripheral blood leukocytes *in vitro*.

MATERIAL AND METHODS

Production of HPV16 L1/L2 VLPs

The production of VLPs was carried out throughout the recombinant protein expression HPV16 L1 and L2 in epithelial human cells of the HEK293T lineage, cultured as previously described (14). Transfection of these cells occur in a transient way using pUF3L1h and pUF3L2h vectors, which are regulated by the human cytomegalovirus promoter containing complete sequences of genes L1 and L2 – a method already described in detail (14, 15). In this study, besides being used to produce VLPs containing both capsid proteins, HEK293T cell line was also used as a control factor on interaction assays with human peripheral blood leukocytes. All assays performed in this study were analysed in duplicate, being representative of at least four independent tests.

Blood collection

Blood samples from 10 healthy female volunteers, ages ranging from 35 to 55, were requested based on epidemiological data associated with genital HPV infection (16). The screening of the volunteers was based on recent blood, Pap smears and colposcopy tests and on data filled out by the candidate on a written informed consent form and on a questionnaire, for the purpose of laboratory research. Volunteers who did not present Pap and colposcopy results within reference values were dismissed. Blood samples were collected in sterile tubes containing heparin – for interaction assays with leukocytes – and EDTA – for blocking assays – , and were processed quickly, within a maximum of 2-hours after collection. During this interval, they were stored at 4^{o}C.

Leukocytes' separation

Whole blood was collected in heparin at a concentration of 0.1 mg/ml, centrifuged at 1,000 rpm for 7 minutes at 5°C in a Sorvall® RT 6000 Refrigerated Centrifuge (Du Pont, Wilmington-DE, USA) with a horizontal angle rotor. The plasma supernatant containing platelets and leukocytes was gently removed and transferred with the aid of a Pasteur pipette to a new tube. An aliquot was collected for total and differential counts, performed in a Neubauer chamber, diluted (ratio 1:1) in Trypan blue and smears were stained by May-Grünwald-Giemsa in order to determine their composition. Leukocytes sedimented were centrifuged again at 1,200 rpm, for 3 minutes, at 5°C, to remove platelets. Leukocytes precipitates were resuspended in 0.85% saline solution for subsequent tests (17). The Neubauer chamber counts and smears containing distinct cell types were analysed by light microscopy, with a Leica DMIL I microscope (Leica Microsystems GmbH, Vienna, AUT).

Interaction assays of HEK293T cells and HPV16 L1/L2 VLPs

HEK293T cells ($2x10^4$ cells/ml) were plated and maintained under growth conditions, washed with PBS and incubated with 120 µg of VLPs in DMEM without FBS, for 4-hours at 37°C and 5% CO_2. After this, cells were washed twice with PBS for 3 minutes each in order to remove non-interactive particles. Cells were then fixed with 2%PFA (Paraformaldehyde, Sigma-Aldrich) in PBS for 1-hour, at 4°C, and washed three times with PBS, 5 minutes each. Plates were kept at 4°C until immunofluorescence assays. Controls were performed in the absence of VLPs and/or the denaturation thereof, by heating at 100°C for 10 minutes (18, adapted).

Interaction assays of human leukocytes and HPV16 L1/L2 VLPs

Leukocytes ($2x10^4$ cells/ml) of healthy volunteers were incubated with 120 µg of VLPs produced in this study and RPMI without FBS for 4-hours at 37°C and 5% CO_2, under gentle agitation. Cells were centrifuged at 1,000 rpm for 7 minutes and cell pellets washed three times with PBS, 5 minutes each. Then, cells were fixed with 2% PFA in PBS for 1-hour, at 4°C. After this step, the centrifugation and PBS washing processes were repeated. Samples were kept at 4°C until immunofluorescence assays. Controls were the same as described above for HEK293T cells.

Interaction assays of leukocytes, transferrin and HPV VLPs

The same protocol described above was employed, with minor changes described below. Leukocytes were incubated with 120 µg of VLPs in separate samples, as follows: the HPV16 L1/L2 VLPs produced in this study, and L1 VLPs of HPV6, 11, 16 and 18 from Gardasil® vaccine, used as control, kindly provided by Merck Sharp & Dohme. RPMI without FBS, together with transferrin (Tf) conjugated to fluorochrome TexasRed® (Molecular Probes™), were added (ratio 1:60, Tf:RPMI). Samples were kept for 15, 45, 60 and 120 minutes in an incubator at 37°C and 5% CO_2, under gentle agitation. The other procedures remained unchanged.

Blocking assays for membrane receptors

Leukocytes of healthy donors were counted and incubated in RPMI medium overnight over coverslips containing poly-L-lysine (Sigma-Aldrich), at 37°C and 5% CO_2. Then, cells were washed and a fresh medium was placed together with specific biochemical inhibitors of ligand uptake (Table 1), used isolated or associated, and incubated for 2 hours (18). After incubation, cells were washed and 120 µg of HPV16 L1/L2 VLPs (19) were added and

incubated with medium for 4 hours. Cells were washed again and fixed in 2% PFA solution. Immunofluorescence assays were carried out to detect the VLP-PBMC interaction by confocal microscopy, using specific antibodies to recognise L1 and L2 proteins. Z-axis 3D images were obtained to confirm the presence of VLPs within cells.

Immunofluorescence assays for internalisation analysis

Leukocytes were washed and fixed as already described. Samples were incubated in PBS containing 1% BSA for 5 minutes under gentle agitation. Later, cells were incubated with the primary antibodies (suppl. Data – Table 1); diluted in PBS containing 0.01% Tween® 20 and 0.5% BSA – pH 8 – for 2 hours, under gentle agitation, at room temperature. They were then washed three times with PBS for 10 minutes each, followed by incubation with the corresponding secondary antibodies (suppl. Data – Table 2); conjugated with fluorochromes; and diluted in PBS containing 0.01% Tween® 20 and 1.5% BSA for 1 hour, under light stirring, at room temperature. Once more, they were washed three times with PBS for 10 minutes each. Samples of leukocytes with transferrin and VLPs were labelled with Phalloidin conjugated AlexaFluor® 594, incubated for 20 minutes. Immediately after that, they were rinsed twice with PBS for 10 minutes each. Aliquots of cell suspension from both items assayed were adhered over silanized slides, and mounted with 5 µl Mowiol® and coverslips. Samples were kept at 4°C until CLSM analysis, using Confocal Laser Scanning Microscope Zeiss 510 Meta of the Butantan Institute (FAPESP Process No. 2000/11624-5; Carl Zeiss GmbH, Jena, DEU).

RESULTS

Leukocytes' identification

After isolation of leukocytes from healthy donors, control smears stained by May-Grünwald-Giemsa method showed cell morphology preservation (17), presenting a positive correlation with the control blood smears. Counts indicated approximately 98% lymphocytes; 0.7% monocytes; 1.5% polymorph nuclear cells; 0.1% red blood cells and 0.1% platelets. The ultrastructure was well preserved for all cell types analysed, with well-defined and intact membranes (17). The efficiency and speed of the method for obtaining leukocytes, preserving morphology and cell viability was confirmed.

Analysis of interaction between HEK293T cells and HPV16 L1/L2 VLPs

HEK293T cells interaction with HPV16 L1/L2 VLPs was analysed by immunofluorescence. We emphasize that the genome of this cell line does not contain any HPV DNA sequences, but it contains Adenovirus DNA and SV40 T-Ag. After 4-hours at a 37^{o}C interaction, cells were washed in order to remove any particles or proteins that did not interacted with HEK293T cells. Then, cells were fixed and stained with the primary antibody Camvir-1 (BD Biosciences – suppl. Data – Table 1) for L1 proteins and with L1 conformation-specific anti-VLP antiserum (Biodesign – suppl. data – Table 1). It was therefore possible to observe the internalisation of VLPs in some cells. In these cells VLPs were found in the cytoplasm, near the core region (suppl. data – Img. 1 A-D), stained with anti-VLP. These results were confirmed by the overlap of images (suppl. data – Img. 1 A and C), and by the most thoroughly detailed internalisation display on the Z-axis scanning sections (suppl. data – Img. 1 B and D). The morphological evaluations show that probably the VLPs' internalisation occurs simultaneously with a large number of particles, similar to the formation of endocytic vesicle structures (suppl. data – Img. 1 C, white arrow). These results suggest that after 4 hours, structured VLPs (suppl. data – Img. 1 A-D), as well as

non-structured VLPs – such as pentameric and monomeric forms of L1 stained with Camvir-1 (suppl. data – Img. 1 E) – , were internalised in epithelial cells from the human kidney (HEK293T), across the cell membrane (suppl. data – Img. 1 B and D). The negative controls showed no immunostaining for L1 and VLPs and no changes in cell morphology were detected (suppl. data – Img. 2).

Analysis of interactions between human leukocytes and HPV16 L1/L2 VLPs

L1/L2 particles were added to human leukocytes, for 4-hours at 37^{o}C, and prepared for indirect CLSM immunofluorescence analysis, in order to investigate the possibility of interaction between the leukocytes and the HPV16 L1/L2 VLPs. Results indicate an interaction of VLPs with peripheral blood mononuclear cells (PBMC) – T and B lymphocytes and monocytes – from healthy women volunteers (Fig. 1). Structured HPV16 L1/L2 VLPs also interacted with and were internalised by leukocytes (Figs. 2 and 3). After 4-hours of interaction, in most leukocytes examined, these particles were found in the cell cytoplasm, as was the case with HEK293T. These results were confirmed by the images' overlap (Figs. 1 A, B and D; Figs. 2 and 3), and the detailed internalisation, as shown on the Z-axis scanning sections (Fig. 2 C). Fig. 1 C (green arrow) shows VLPs across the cell membrane. The Z-axis' sweep cuts were able to demonstrate the internalisation of the VLP with a larger number of particles similar to the formation of endocytic vesicles structures (Fig. 2 A, white arrow), like those found in HEK293T cells (suppl. data – Img. 1 C, white arrow), a phenomenon endorsed by morphological evaluations. In Fig. 3, the interaction of leukocytes with the VLPs is illustrated, showing the colocalisation of HPV16 L1/L2 proteins recognised by anti-L1 (green) and anti-L2 (red), respectively. This colocalisation was expected in VLPs that are composed of these two proteins, as it might be seen from the

images' overlap (Fig. 3). Fig. 3 B shows the internalisation of VLPs by leukocytes in a significant amount when compared to other interactions. At least 15 fields were analysed per experiment, containing from 4 to 10 cells per field. The presence of structures similar to vacuoles can also be observed (Fig. 3 B, blue arrow). Control assays showed no immunostaining, neither with the antibodies used to detect L1 and L2 separately, nor with structured HPV16 L1/L2 VLPs (suppl. data – Img. 3).

Identification of human PBMC interactions with VLPs

These cells were treated with antibodies in order to recognise specific cell membrane receptors for each type (suppl. data – Table 1), and analysed by indirect immunofluorescence using CLSM to identify PBMC interactions with HPV16 VLPs, after 4-hours incubation at 37^{o}C. HPV16 VLPs interacted with *ex vivo* PBMC (Figs. 4-6). These results were confirmed by the images' overlap (Figs. 4 and 5) and displayed detailed internalisation on the Z-axis sections (Fig. 6). T and B lymphocytes showed greater competence to internalise VLPs, at around 47%-52% of cells (Table 2). Through morphological assessments, T-lymphocytes that internalised VLPs and were recognised by anti-CD8 showed endocytic vesicles-like structures (Fig. 4 B, white arrow). Only 23% of monocytes that were identified by anti-CD14 antibody interacted with the VLPs (Table 2).

Analysis of the colocalisation of VLPs and transferrin (Tf) in human PBMC

After 15 minutes, no colocalisation between L1 VLPs and exogenous Tf was detected (Fig.7). Moreover, it was possible to show the internalisation of VLPs during this period. After 45 minutes, colocalisation of VLPs with exogenous Tf in the cytoplasm of human PBMC (Fig. 8 and 9, yellow arrows), and also with the TfR or CD71, was observed (Fig. 9

A-B, yellow arrows) suggesting that the iron pathway may be used to HPV internalisation. All results were confirmed by the images' overlap, respectively (Figs. 7-9).

We compared the kinetics of internalization of Tf and TfR (CD71) with the colocalisation of HPV16 L1/L2 VLPs produced in this study and with control HPV6, 11, 16, 18 L1 VLPs derived from the Gardasil® vaccine (Fig. 10). After only 15 minutes of interaction it was possible to observe colocalisation of TfR and Tf (Fig. 10 A-B, purple arrows) with both L1/L2 VLPs (Fig. 10 A) as well as with Gardasil L1 VLPs (Fig. 10 B). By means of morphological analysis, we were able to demonstrate the colocalisation of both VLPs – L1 and L1/L2 – with Tf and TfR in the leukocytes' cytoplasm, after a 45-minutes interaction period (Fig. 10 C-D, white arrows). This colocalisation among VLPs, Tf and TfR was found in approximately 50% of analysed cells. Within 60 minutes of interaction, we observed a feeble colocalisation between Tf and VLPs in about 30% of the cells (Fig. 10 E-F, orange arrows). No colocalisation was observed in the tests after 120 minutes. The colocalisation was evidentiated in detail by three-dimensional figures stacked in Z-axis (Fig. 10). The negative controls showed no signs of L1 and VLPs. However, it was possible to observe exogenous Tf internalisation (suppl. data – Img. 4). Comparative testing of L1/L2 VLPs produced in this study and of control L1 VLPs from Gardasil® vaccine showed no significant differences in the analysed results.

Analysis of the blocking assays of PBMC membrane receptors

After successful identification of VLPs within leukocytes and their colocalisation with Tf and TfR, a variety of biochemical inhibitors, known to inhibit distinct cellular processes, was used to demonstrate the involvement of these and other different pathways of VLPs entry in PBMC.

Chlorpromazine inhibits clathrin-mediated endocytosis of various plasma membrane proteins. Nystatin is a sterol-binding agent that disassembles caveolae in the membrane. rCTB (Clostridium toxin B) acts by shortening the actin filaments' length, by inhibiting its process *in vitro*. Liquemin is related with the VLPs obstruction of internalisation through the HSPG (Heparan sulphate proteoglycans) pathway. Sodium azide is an ATPase inhibitor, which blocks particle movement towards the cell body and leads to a diffuse random movement.

The use of these different biochemical inhibitors was not sufficient to block the HPV16 L1/L2 VLPs entry in the PBMC (Figs. 11-12). Chlorpromazine – although known for blocking the clathrin pathway through CD71 receptor of Tf – was not able to inhibit VLPs entrance inside PBMC in a satisfactory manner. The same occurred when rCTB, Filipin and Nystatin, Liquemin and Sodium azide were used to block actin-dependent cell processes, the caveolae pathway, the HSPG pathway, and endocytic pathways, respectively, either assayed separately or associated in an all-inhibitors cocktail. These results suggest that PBMC makes use of multiple internalisation pathways to uptake HPV16 particles.

DISCUSSION

Differently of many Beta and Gamma papillomavirus, Alpha papillomaviruses developed immune system evasion strategies from the host, causing persistent and visible papillomas, which sometimes evolving to cancers (20). Some HPV types including 16, 18, 31, 33, 35, 39, 45, 51, 52, 56, 58 and 59 have been classified as human carcinogens by the IARC, being responsible for at least 4% of all human malignancies (4, 21, Papillomavirus Episteme (PaVE); http://pave.niaid.nih.gov/#home). Infection by high-risk HPV types is the major factor for the development of cervical cancer, and HPV DNA is also found in

359 tumours affecting other anogenital regions. Besides, they are being correlated with an
360 increasing proportion of oropharyngeal squamous cells carcinomas, and occurrences
361 affecting mainly tonsil and base of tongue regions are currently being documented in
362 particular geographic areas (22). A study describes women who have never experienced
363 sexual intercourse as having genital lesions caused by HPV, showing that, in addition to
364 sexual transmission, could have other forms of infection such as fomites and skin contact,
365 and maternal-foetal vertical transmission is also being considered as a probable infection
366 pathway (23-27).
367 Cell-virus interaction is the initial step in viral infection. Often, virus adsorption occurs on
368 the plasma membrane of susceptible cells. In general, the most common solution is that the
369 pathogen's intracellular trafficking occurs through and existing entry mechanism, mediated
370 via clathrin, caveolin, macropinocytosis, among others, moving inside cells to reach the
371 location where viral replication occurs (28). Transcytosis is used to move antigens and
372 protective antibodies across epithelial barriers. Similar to what seems to occur with HIV
373 (29), the transcytosis of HPV through epithelial cells, crossing cellular barriers, should also
374 be dependent on trafficking to the endocytic recycling pathway. The productive life cycle
375 of HPV is directly linked to epithelial differentiation. It is believed that the papillomavirus
376 is capable of maintaining the expression of structural genes, under tight control of the
377 regulatory mechanisms of transcription and translation (30). The L1 capsid protein of HPV,
378 regardless of the presence or absence of L2, has the property of forming structures that
379 mimic morphologically authentic virions, VLPs, which are being used as replacements for
380 HPV infected cell culture *in vitro* (8, 14, 31, 32). However, the presence of L2 seems to
381 confer greater stability to the virus and VLP, therefore, the viral capsid indeed seems to
382 contribute to the virus' infectivity (33). Most experimental models explore the process of

383 host cell interaction by molecular or biochemical methods, using cell lines from different
384 tissues and species in interactions with HPV L1 VLPs in their studies.
385 In the present work, we produced HPV L1/L2 VLPs (14, 15) to investigate the possibility
386 that these particles interact with human leukocytes, in order to understand possible
387 mechanisms involved in these interactions. We have developed a method for the isolation
388 of these cells (17), used in suspension at 37^{o}C, thereby creating an *ex vivo* system as closely
389 as possible to the natural conditions of HPV16 infection, thus conceiving a novel
390 experimental model.
391 HPV16 recombinant proteins L1, L2 and VLPs were visualized in the perinuclear region of
392 HEK293T cells, in compliance with data described in the literature (34). The presence of
393 BPV (bovine papillomavirus) in lymphocytes has been discussed (35, 36). Using PCR
394 technique (Polymerase Chain Reaction) in samples taken from humans with anogenital
395 lesions, the presence of HPV16 in peripheral blood samples (37) and in plasma cells (38)
396 was detected. Besides, DNA of other HPV types has been found in PBMC (39, 40). The
397 presence of HPV in lymphocytes of patients treated for anogenital cancers suggests that the
398 virus can remain in these cells even after treatment. However, there are no convincing
399 evidences that support that lymphocytes carry/produce infectious HPV viral particles.
400 Nonetheless, the presence of HPV macromolecules in lymphocytes may play a role in viral
401 immune response.
402 The scientific literature discloses that papillomavirus exhibits specific tropism for species
403 and tissues. However, BPV1 particles, isolated from bovine warts, and HPV16 VLPs
404 interacted successfully with 14 cell lines derived from different species and tissues, as
405 demonstrated in two different studies (32, 41). Using our model to investigate this, HPV16
406 L1/L2 VLPs interacted *in vitro* and *ex vivo* with two very distinct human cells, epithelial

kidney cells and PBMC, respectively. After 4 hours of interaction, these particles' internalisation occurred, showing a very similar distribution pattern on both cell types. In both, L1 VLPs were located in the cytoplasm near the nucleus, suggesting that tissue differences do not affect the ability of HPV16 VLPs to entry in different cell types, and that pentameric and monomeric forms of L1 may also be internalised. The interaction between VLPs and monocytes observed in this study showed colocalisation with CD14. As macrophage precursors, apparently these cells are able to internalise particles at a much larger amount if compared with lymphocytes. The unexpected colocalisation of CD14 membrane receptor and VLPs, as well as the morphological changes observed, suggest that monocytes respond to this interaction as immune cells, in order to eliminate invading microorganisms. CD14 is a 53-kDa molecule, expressed mainly in monocytes, macrophages and granulocytes. It is also found as soluble protein in the serum (42). One known function of this receptor is to bind the complex of LPS (bacterial lipopolysaccharide). Macrophages expressing CD14 can respond to very small amounts of LPS, and this interaction is required for activation of these cells (43). Some studies suggest that the receptor CD16 (FcγRIII), present on the plasma membrane surface of neutrophils, can bind to VLPs at mice splenocytes' surface, indicating that this receptor has a role to play in immune response against viral capsid proteins (43, 44). It is necessary to clarify the actual mechanisms involved in the interactions between CD14, CD16 and VLPs, in order to better understand how the immune system can properly eliminate the HPV from the host. Tf is a beta globulin responsible for the transport of iron (Fe), through plasma, to the interior of cells. Besides hepatocytes, other cells in the body are able to synthesize it. The TfR is a membrane protein expressed primarily in T and B lymphocytes, macrophages, and proliferating cells such as homodimers with N-terminal cytoplasmic tails (42). TfR is

431 constantly being endocytosed by plasma membrane through clathrin-mediated endocytosis,
432 with the purpose of carrying ferric iron bound to Tf to the inside of cells. This Tf-TfR
433 complex is delivered to the early endosome into a lower pH medium, where iron is released
434 and TfR is recycled to the cell's surface (45). When evaluating the interactions between
435 HPV16 L1/L2 VLPs, HPV6, 11, 16, 18 L1 VLPs (Gardasil® vaccine) and unstructured
436 HPV16 L1 in PBMCs and in the presence of exogenous Tf, we determined the
437 colocalisation of L1-VLP-Tf and free Tf in these cells, as well as colocalisation with TfR,
438 after 45 minutes of interaction. This colocalisation between VLP, Tf and TfR was found in
439 approximately 50% of analysed cells. These results suggest that HPV16 L1/L2 VLPs,
440 HPV6, 11, 16, 18 L1 VLPs (Gardasil® vaccine) and unstructured HPV16 L1 can enter cells
441 by endocytosis through clathrin-dependent, via TfR. It is probable that, along viral infection
442 processes, interactions between HPV16 (about 55 nm size) and Tf molecules (80-kDa)
443 might indeed happen, through fusion with Fe-Tf-TfR complexes, mimicking its entry into
444 the cell via low pH endosomes, thus enabling transcytosis (29, 46-49).
445 There have been no reports in the literature showing the internalisation of HPV VLPs in
446 human PBMC. So far, this study has showed that PBMCs of healthy female volunteers
447 were able to internalise HPV16 VLPs. Also, T and B Lymphocytes were the main cell
448 types that further interacted with VLPs. It is important to emphasize that the lymphocytes
449 are cells capable of dividing themselves and it is estimated that the half-life of these
450 inactive cells in humans is of some years. Furthermore, inactive lymphocytes circulate
451 continuously through the bloodstream and lymphatic vessels. Using different cell lineages
452 with VLPs or PsV (pseudovirion), scientists have come to different conclusions. Our
453 findings agree with the data obtained by other researchers who – through the use of PsV-
454 infected HeLa and HaCaT cells – successfully demonstrated that the HPV entry is clathrin-

455 caveolin-cholesterol-and-dynamin-independent (7). The entry of HPV VLPs in leukocytes
456 by independent endocytosis pathways may be due to their ability to recognise, capture and
457 remove foreign substances from the body. The use of different biochemical inhibitors,
458 isolated or associated, does not seem to be enough to block the internalisation of HPV16
459 L1/L2 VLPs in the PBMC, suggesting that a specific receptor is not required to the uptake
460 and HPV16 entry into the host cells. A recent study demonstrates that intrinsic risk factors
461 are responsible of around 10%-30% of cancer development risk, and that the rates of
462 endogenous mutation accumulation by intrinsic processes are not sufficient to account for
463 the high cancer risks observed. Cancer risk in general is heavily influenced by extrinsic
464 factors like HPV infection (50). Unravelling the molecular steps leading to virus entry into
465 the cells may be important for the development of new strategies for the prevention of
466 infection by HPV and foster immune response against important human pathogen.
467

468 **CONCLUSIONS**

469 HPV16 L1/L2 VLPs produced in this study interacted with *in vitro* HEK293T cells and *ex*
470 *vivo* PBMC from healthy women volunteers, and were internalised. This study evinced that
471 HPV16 L1/L2 VLPs can interact with the plasma membrane surface, and been uptake by
472 lymphocytes. We also demonstrated that HPV16 L1/L2 VLPs might utilize the endocytic
473 pathway of iron-mediated clathrin as a receptor, which involves multiple membrane
474 receptors simultaneously and also the classical endocytic pathway of iron – the most
475 widespread among vertebrates and the animal kingdom as a whole – we have demonstrated
476 that HPV16 L1/L2 VLPs does not require a specific receptor in order to be internalised by
477 leukocytes. Complementary studies are required to accurately demonstrate the probable
478 mechanisms involved.

ACKNOWLEDGEMENTS

The authors would like to express their deepest gratitude to the CAPES Master's Degree Fellowship to V. Szulczewski and E.A. Kavati, from the Biotechnology Interunits Postgraduate Programme USP-IBU-IPT; PAP-SES-FUNDAP Fellowships to T.M. Hosoda; Financial Support: FAPESP – Process Number 2004/15122-5; Butantan Foundation and Butantan Institute; to the Prof Dr Richard B.S. Roden, from the Department of Pathology, Johns Hopkins University, Baltimore, MD, USA, which kindly provided us anti-L2 antibody, and for useful comments on the manuscript.

Ethical Committee

This work was duly evaluated and approved by the Sao Joaquim Hospital, Real and Meritorious Portuguese Beneficence Association Ethical Committee on Human Research. Protocol number: 369-08.

This work is in full compliance with the National Biosafety Law (CTNBio) guidelines and the present study was approved by the Butantan Institute Institutional Biosafety Committee (CIBio) and CTNBio – Process Nr. 01200.004893/1997-93 – published in the Brazilian Official Gazette (DOU) on August 16, 2011.

REFERENCES

1. **zur Hausen H, Meinhof W, Scheiber W, Bornkamm GW.** 1974. Attempts to detect virus-specific DNA sequences in human tumors: I. Nucleic acid hybridizations with complementary RNA of human wart virus. Int J Cancer **13:**650-

656. (First negative attempt to find papillomavirus DNA in cancer of the cervix with labelled HPV DNA from plantar warts).

2. **zur Hausen H.** 1976. Condylomata acuminata and human genital cancer. Cancer Res **36:**794. (Hypothesis that papillomaviruses are involved in the etiology of cancer of cervix).

3. **Dürst M, Dzarlieva-Petruseyska RT, Boukamp P, Fusenig NE, Gissmann L.** 1987. Molecular and cytogenetic analysis of immortalized human primary keratinocytes obtained after transfection with human papillomavirus type 16 DNA. Oncogene **1:**251-256.

4. **Viarisio D, Gissmann L, Tommasino M.** 2017. Human papillomaviruses and carcinogenesis: well-established and novel models. Curr Opin Virol **26:**56-62.

5. **Sanjosé S, Serrano B, Castellsagué X, Brotons M, Muñoz J, Bruni L, Bosch FX.** 2012. Human papillomavirus (HPV) and related cancers in the Global Alliance for Vaccines and Immunization (GAVI) countries. AWHO/ICO HPV Information Centre Report. Vaccine **30S:**D1-D83.

6. **Day PM, Lowy DR, Schiller JT.** 2003. Papillomaviruses infect cells via a clathrin-dependent pathway. Virology **307:**1-11.

7. **Raff AB, Woodham AW, Raff LM, Skeate JG, Yan L, Da Silva DM, Schelhaas M, Kast WM.** 2013.The evolving field of human papillomavirus receptor research: a review of binding and entry. J Virol **87:**6062-6072.

8. **Bousarghin L, Touzé A, Combita-Rojas AL, Coursaget P.** 2003. Positively charged sequences of human papillomavirus type 16 capsid proteins are sufficient to mediate gene transfer into target cells via the heparan sulfate receptor. J Gen Virol **84:**157-164.

9. **Hindmarsh PL, Laimins LA.** 2007. Mechanisms regulating expression of the HPV 31 L1 and L2 capsid proteins and pseudovirion entry. Virol J **4:**1-12.

10. **Bosch FX, Broker TR, Forman D, Moscicki AB, Gillison ML, Doorbar J, Stern PL, Stanley M, Arbyn M, Poljak M, Cuzick J, Castle PE, Schiller JT, Markowitz LE, Fisher WA, Canfell K, Denny LA, Franco EL, Steben M, Kane MA, Schiffman M, Meijer CJ, Sankaranarayanan R, Castellsagué X, Kim JJ, Brotons M, Alemany L, Albero G, Diaz M, Sanjosé S**. 2013. Authors of ICO Monograph Comprehensive Control of HPV Infections and Related Diseases. Vaccine **31:**H1-31. Collaborators (98)

11. **Alemany L, Saunier M, Alvarado I, Quirós B, Salmeron J, Shin HR, Pirog E, Guimerà N, Hernández GA, Felix A, Clavero O, Lloveras B, Kasamatsu E, Goodman MT, Hernandez BY, Laco J, Tinoco L, Geraets DT, Lynch CF, Mandys V, Poljak M, Jach R, Verge J, Clavel C, Ndiaye C, Klaustermeier J, Cubilla A, Castellsagué X, Bravo IG, Pawlita M, Quint W, Muñoz N, Bosch FX, Sanjosé S on behalf of the HPV VVAP study group.** 2015. HPV DNA prevalence and type distribution in anal carcinomas worldwide. Int J Cancer **136:**98-107.

12. **Kavati EA, Palumbo ACM, Andrade FB, Marigliani B, Sakauchi D, Leão E, Armbruster-Moraes E, Müller M, Cianciarullo AM.** 2012. Interaction of HPV16L1L2 VLP with stem cells CD34+/CD117+ of the human amniotic fluid. In: Current microscopy contributions to advances in science and technology. Editor: Antonio Méndez-Vilas. Publisher: Formatex Research Center, Badajoz, Spain. Volume **5:**617-624. ISBN-13: 978-84-939843-5-9. http://www.formatex.info/microscopy5/book/617-624.pdf

13. **Dunne EF, Markowitz LE, Saraiya M, Stokley S, Middleman A, Unger ER, Williams A, Iskander J.** 2014. Centers for Disease Control and Prevention. CDC Grand Rounds: Reducing the Burden of HPV-Associated Cancer and Disease. MMWR **63:**69-72.

14. **Cianciarullo AM, Szulczewski V, Chaves AAM, Bazan SB, Aires KA, Müller M, Armbruster-Moraes E.** 2010. Production of HPV16 L1L2 VLPs in cultures of human epithelial cells. In: Microscopy: Science, Technology, Applications and Education. Editors: Antonio Méndez-Vilas and Jesús Díaz Álvarez. Publisher: Formatex Research Center, Badajoz, Spain. Volume **4:**1073-1082. ISBN- 13: 978-84-614-6190. http://www.formatex.info/microscopy4/ 1073-1082.pdf

15. **Marigliani B, Kavati EA, Sakauchi D, Oliveira HB, Canali RA, Sasaki AA, Ferreira Jr JMC, Armbruster-Moraes E, Müller M, Cianciarullo AM.** 2012. Intracellular distribution of recombinant Human Papillomavirus capsid proteins. In: Current microscopy contributions to advances in science and technology. Editor: Antonio Méndez-Vilas. Publisher: Formatex Research Center, Badajoz, Spain. Volume **5:**678-684. ISBN-13: 978-84-939843-5-9. http://www.formatex.info/microscopy5/book/678-684.pdf

16. **Nonnenmacher B, Breitenbach V, Villa LL, Prolla JC, Bozzetti MC.** 2002. Genital human papillomavirus infection identification by molecular biology among asymptomatic women. Rev Saude Publica **36:**95-100.

17. **Kavati EA, Hosoda TM, Szulczewski V, Leão E, Borelli P, Cianciarullo AM.** 2017. A simple, fast, inexpensive and efficient method for leukocytes separation with preservation of morphology and cell viability for use in education and research. In: Microscopy and imaging science: practical approaches to applied research and

573 education. Editor: Antonio Méndez-Vilas. Publisher: Formatex Research Center,
574 Badajoz, Spain. Volume **7:**665-670. ISBN-13: 978-84-942134-9-6.
575 http://www.microscopy7.org/book/665-670.pdf

576 18. **Fothergill T, Mcmillan NAJ.** 2006. Papillomavirus virus-like particles activate the
577 PI3-kinase pathway via alpha-6 beta-4 integrin upon binding. J Virol **352:**319-328.

578 19. **Van Hamme E, Dewerchin HL, Cornelissen E, Verhasselt B, Nauwynck HJ.**
579 2008. Clathrin- and caveolae-independent entry of feline infectious peritonitis virus
580 in monocytes depends on dynamin. J Gen Virol **89:**2147-2156.

581 20. **Doorbar J, Egawa N, Griffin H, Kranjec C, Murakami I.** 2015. Human
582 papillomavirus molecular biology and disease association. Rev Med Virol **25:**2-23.

583 21. **Schellenbacher C, Roden RBS, Kimbauer R.** 2017. Developments in L2-based
584 human papillomavirus (HPV) vaccines. Virus Res **231:**166-175.

585 22. **Näsman A, Nordfors C, Holzhauser S, Vlastos A, Tertipis N, Hammar U,**
586 **Hammarstedt-Nordenvall L, Marklund L, Munck-Wikland E, Ramqvist T,**
587 **Bottai M, Dalianis T.** 2015. Incidence of human papillomavirus positive tonsillar
588 and base of tongue carcinoma: a stabilisation of an epidemic of viral induced
589 carcinoma? Eur J Cancer **51:**55-61.

590 23. **Frega A, Cenci M, Stentella P, Cipriano L, De Ioris A, Alderisio M, Vecchione**
591 **A.** 2003. Human papillomavirus in virgins and behaviour at risk. Cancer Lett **194:**
592 21-24.

593 24. **Armbruster-Moraes E, Ioshimoto LM, Leão E, Zugaib M.** 1994. Presence of
594 human papillomavirus DNA in amniotic fluids of pregnant women with cervical
595 lesions. Gynecol Oncol **54:**152–158.

25. **Rombaldi RL, Serafini EP, Mandelli J, Zimmermann E, Losquiavo KP.** 2008. Transplacental transmission of human papillomavirus. Virol J **5:**106.

26. **Sarkola ME, Grénman SE, Rintala MA, Syrjänen KJ, Syrjänen SM.** 2008. Human papillomavirus in the placenta and umbilical cord blood. Acta Obstet Gynecol Scand **87:**1181-1188.

27. **Koskimaa HM, Waterboer T, Pawlita M, Grénman S, Syrjänen K, Syrjänen S.** 2012. Human papillomavirus genotypes present in the oral mucosa of newborns and their concordance with maternal cervical human papillomavirus genotypes. J Pediatr **160:**837-843.

28. **Gruenberg J, van der Goot FG.** 2006. Mechanisms of pathogen entry through the endosomal compartments. Nat Rev Mol Cell Biol **7:**495-504.

29. **Kinlock BL, Wang Y, Turner TM, Wang C, Liu B.** 2014. Transcytosis of HIV-1 through vaginal epithelial cells is dependent on trafficking to the endocytic recycling pathway. PLoS ONE **9:**e96760.

30. **Müller M.** 2005. Human Papilloma Viruses: Methods and Protocols. Humana Press Inc. In: Davy, C.; Doorbar, J. Methods in Molecular Medicine. Totowa, NJ. **119:**435-446.

31. **Müller M, Gissmann L, Cristiano RJ, Sun XY, Frazer IH, Jenson AB, Alonso A, Zentgraf H, Zhou J.** 1995. Papillomavirus capsid binding and uptake by cells from different tissues and species. J Virol **69:**948-954.

32. **Roden RB, Kirnbauer R, Jenson AB, Lowy DR, Schiller JT.** 1994a. Interaction of papillomaviruses with the cell surface. J Virol **68:**7260-7266.

33. **Kieback E, Müller M.** 2006. Factors influencing subcellular localization of the human papillomavirus L2 minor structural protein. Virology **345:**199-208.

620 34. **Leder C, Kleinschmidt JA, Wiethe C, Müller M.** 2001. Enhancement of Capsid
621 Gene Expression: Preparing the Human Papillomavirus Type 16 Major Structural
622 Gene L1. J Virol **75:**9201-9209.
623 35. **Campo MS, Jarrett WF, Barron R, O'Neil BW, Smith KT.** 1992. Association of
624 bovine papillomavirus type 2 and bracken fern with bladder cancer in cattle. Cancer
625 Res **52:**6898-6904.
626 36. **Stocco dos Santos RC, Lindsey CJ, Ferraz OP, Pinto JR, Mirandola RS, Benese**
627 **FJ, Birgel EH, Bragança-Pereira CA, Beçak W.** 1998. Bovine papillomavirus
628 transmission and chromosomal aberrations: an experimental model. J Gen Virol
629 **79:**2127-2135.
630 37. **Tseng CJ, Lin CY, Wang RL, Chen LJ, Chang YL, Hsieh TT, Pao CC.** 1992.
631 Possible transplacental transmission of human papillomaviruses. Am. J. Obstet
632 Gynecol **166:**35-40.
633 38. **Payne D, Tyring SK, Doherty MG, Daya D, Chan TS.** 1993. Detection of human
634 papillomavirus type 16 in plasma cells. Gynecol Oncol **48:**406-412.
635 39. **Pao CC, Lin SS, Lin CY, Maa JS, Lai CH, Hsieh TT.** 1991. Identification of
636 human papillomavirus DNA sequences in peripheral blood mononuclear cells. Am J
637 Clin Pathol **95:**540-546.
638 40. **Karas Z, Porebas E.** 1998. HPV sequences in blood of patients with condyloma
639 acuminata. J Invest Dermatol **110:**843-844.
640 41. **Roden RB, Weissinger EM, Henderson DW, Booy F, Kirnbauer R, Mushinski**
641 **JF, Lowy DR, Schiller JT.** 1994b. Neutralization of bovine papillomavirus by
642 antibodies to L1 and L2 capsid proteins. J Virol **68:**7570-7574.

643 42. **Abbas AK, Lichtman AH.** 2005. Cellular and Molecular Immunology. 5 ed.
644 Philadelphia: Elsevier, 580 p.
645 43. **Da Silva DM, Velders MP, Nieland JD, Schiller JT, Nickoloff BJ, Kast WM.**
646 2001. Physical interaction of human papillomavirus virus-like particles with immune
647 cells. Int Immunol **13:**633-641.
648 44. **Da Silva DM, Fausch SC, Verbeek JS, Kast WM.** 2007. Uptake of human
649 papillomavirus virus-like particles by dendritic cells is mediated by Fc gamma
650 receptors and contributes to acquisition of T cell immunity. J Immunol **178:**7587-97.
651 45. **Trowbridge IS, Omary MB.** 1981. Human cell surface glycoprotein related to cell
652 proliferation is the receptor for transferrin. Proc Natl Acad Sci USA **78:**3039–3043.
653 46. **Tuma PL, Hubbard AL.** 2003. Transcytosis: crossing cellular barriers. Physiol Rev
654 **83:**871-932.
655 47. **Kinlock BL, Wang Y, Turner TM, Wang C, Liu B.** 2014. Transcytosis of HIV-1
656 through vaginal epithelial cells is dependent on trafficking to the endocytic recycling
657 pathway. PLoS One **9:**e96760.
658 48. **Anderson DJ.** 2014. Modeling mucosal cell-associated HIV type 1 transmission in
659 vitro. J Infect Dis **210:**S648-S653.
660 49. **Sakajiri T, Yamamura T, Kikuchi T, Yajima H.** 2009. Computational structure
661 models of apo and diferric transferrin-transferrin receptor complexes. Protein J
662 **28:**407-414.
663 50. **Wu S, Powers S, Zhu W, Hannun YA.** 2016. Substantial contribution of extrinsic
664 risk factors to cancer development. Nature **529:**43-47.
665
666

667 **Figure Legends**

668 **Figure 1:** Interactions of human leukocytes with VLPs of HPV16, detected by indirect
669 immunofluorescence. The leukocyte cells were incubated with the VLPs for 4 h. Following
670 fixation, they were immunostained with anti-HPV16 L1 antibody and then stained with a
671 secondary antibody conjugated to FITC (green). In all assays, AlexaFluor® 594-conjugated
672 Phalloidin (red) detected the actin cytoskeleton. The internalisation of VLPs (green arrows)
673 is shown in image C, through the sweep cuts on the Z-axis (C) 9.50 µm thick sections and
674 each section to 1.60 µm. CLSM Zeiss LSM 510 Meta. Magnification: Objective C-
675 Apochromatic 63xs /1.4 oil. Bar = 5 µm.

676

677 **Figure 2:** Interactions of human leukocytes with VLPs of HPV16, detected by indirect
678 immunofluorescence. The leukocyte cells were incubated with the VLPs for 4 h. Following
679 fixation, they were immunostained with the conformational anti-HPV16 VLPs and stained
680 with a secondary antibody conjugated to FITC (green). AlexaFluor® 594-conjugated
681 Phalloidin (red) detected the actin cytoskeleton. The internalisation of VLPs (green arrows)
682 is shown in image C, through Z-axis sweep cuts (C) 7.80 µm thick sections and each
683 section to 1.30 µm. In (A) we see a structure similar to an endocytic vesicle (white arrow).
684 CLSM Zeiss LSM 510 Meta. Magnification: Objective C-Apochromatic 63xs /1.4 oil. Bar
685 = 5 µm.

686

687 **Figure 3:** Interactions of human leukocytes with VLPs of HPV16, detected by indirect
688 immunofluorescence. After fixation, cells were immunostained with anti-HPV16 L1
689 antibody and then stained with a secondary antibody conjugated to FITC (green). Then
690 immunostained with anti-HPV16 L2 antibody and revealed by AlexaFluor®555 secondary

antibody (red). The internalisation of VLPs (yellow arrows) is shown in confocal images (merge). In (B) structures similar to vacuoles (blue arrow) might be observed. CLSM Zeiss LSM 510 Meta. Magnification: Objective C-Apochromatic 63xs /1.4 oil. Bar = 5 µm.

Figure 4: Identification of human leukocyte interactions with the HPV16 VLPs analysed by indirect immunofluorescence. After fixation, cells were immunostained with the conformational anti-HPV16 VLPs and revealed by a secondary antibody conjugated to FITC (green). Then, the cells were treated with anti-CD04 (A) and anti-CD08 (B) and stained with a secondary antibody AlexaFluor®546 (red). VLP internalisation (green arrows) is visible on image overlay (merged images). In (B), a structure similar to an endocytic vesicle is detectable (white arrow). CLSM Zeiss LSM 510 Meta. Magnification: Objective C-Apochromatic 63xs /1.4 oil. Bar = 5 µm.

Figure 5: Identification of human leukocyte interactions with the HPV16 VLPs, analysed by indirect immunofluorescence. After fixation, cells were immunostained with the conformational anti-HPV16 VLPs and revealed by a secondary antibody conjugated to FITC (green). Then, the cells were treated with anti-CD20 and anti-CD14 and stained with a secondary antibody AlexaFluor®546 (red). VLP internalisation (green arrows) is visible on image overlay (merged images). In (B) we can observe the colocalisation of CD14 and VLPs (orange arrow) and vacuole-like structures (blue arrow). CLSM Zeiss LSM 510 Meta. Magnification: Objective C-Apochromatic 63xs /1.4 oil. Bar = 5 µm.

Figure 6: Identification of human leukocyte interactions with the HPV16 VLPs analysed by indirect immunofluorescence. After fixation, cells were immunostained with the

715 conformational anti-HPV16 VLPs and revealed by a secondary antibody conjugated to
716 FITC (green). Then, the cells were treated with anti-CD20 (C), anti-CD04 (A), anti-CD08
717 (B), anti-CD14 (D) and AlexaFluor®546 revealed by secondary antibody (red). VLP
718 internalisation (green arrows) is shown in the images through Z-axis sweep cuts. (A) 9.25
719 µm of thick sections and each section of 0.84 µm; (B) 8.56 µm thick sections and each
720 section with 0.95 µm; (C) 9.27 µm thick sections and each section with 1.03 µm; (D) 10,94
721 µm thick sections and each section having 1.40 µm. CLSM Zeiss LSM 510 Meta.
722 Magnification: Objective C-Apochromatic 63xs /1.4 oil.
723
724 **Figure 7:** Colocalisation of VLPs of HPV16 and Tf in human leukocytes, detected by
725 indirect immunofluorescence. The leukocyte cells were incubated with the VLPs and the
726 conjugated Tf TexasRed® (red). Leukocytes were treated with anti-HPV16 L1 antibody,
727 revealed by a secondary antibody conjugated to FITC (green). In confocality (merge), the
728 images reveal colocalisation of L1 and Tf (yellow arrows). CLSM Zeiss LSM 510 Meta.
729 Magnification: Objective C-Apochromatic 63xs /1.4 oil. Bar = 5 µm.
730
731 **Figure 8:** Colocalisation of HPV16 VLPs and Tf in human white blood cells, detected by
732 indirect immunofluorescence. The leukocyte cells were incubated with the VLPs and the
733 conjugated Tf TexasRed® (red). Leukocytes were immunostained with anti-HPV16 VLP
734 antibody and revealed by a secondary antibody conjugated to FITC (green). In confocality
735 (merge), the images reveal colocalisation of VLPs and Tf (yellow arrows). CLSM Zeiss
736 LSM 510 Meta. Magnification: Objective C-Apochromatic 63xs /1.4 oil. Bar = 5 µm.
737

738 **Figure 9:** Three-dimensional imaging of leukocyte interactions with the VLPs produced in
739 this study or the VLP vaccine Gardasil, Tf and TfR; detected by indirect
740 immunofluorescence. The leukocyte cells were incubated with the VLPs and the conjugated
741 Tf TexasRed® (red). After fixation, the leukocytes were immunostained with anti-HPV16
742 VLP antibody and revealed by a secondary antibody, conjugated to FITC (green), then
743 treated with anti-CD71 and revealed by AlexaFluor®633 (blue). (A) and (B) colocalisation
744 Tf and TfR (purple arrow), (C) and (D) colocalisation VLP / Tf / TfR (white arrows), (E)
745 and (F) weak colocalisation VLP / Tf (orange arrows). CLSM Zeiss LSM 510 Meta.
746 Magnification: Objective C-Apochromatic 63xs /1.4 oil.
747
748 **Figure 10 (1-6):** Immunofluorescence assay detecting the HPV VLPs entry in PBMC, even
749 in presence of specific biochemical inhibitors of ligand uptake: (1) Sodium azide; (2)
750 Chlorpromazine; (3) Liquemin; (4) rCTB; (5) Filipin; (6) Nystatin. (a) shows the overlay
751 (merge) of images detected by stain of L1 protein (green), L2 protein (red), nuclei (blue);
752 (b) Z-axis showing L1 protein within cells; (c) Z-axis showing the entry of L2 protein in
753 cells was not inhibited. CLSM Zeiss LSM 510 Meta. Magnification: Objective C-
754 Apochromatic 63xs /1.4 oil. Bar = 5 µm.
755
756 **Figure 11.** Assay performed with all inhibitors used in Fig.15 (1-6), in association. (a)
757 Detection of L1 protein (green); (b) L2 protein within cells (red); (c) nuclei (blue); (d) the
758 overlay (merge) of images (a, b and c); Z-axis showing the L1 (e) and L2 (f) proteins within
759 cells. CLSM Zeiss LSM 510 Meta. Magnification: Objective C-Apochromatic 63xs /1.4 oil.
760 Bar = 5 µm.
761

762 **Illustrations**

763 **Table 1:** Biochemical inhibitors used to examine their effects on the entry of HPV VLPs in

764 PBMC.

Inhibitors	Inhibition
Chlorpromazine	Clathrin pathway
rCTB (Clostridium toxin B)	Actin-dependent cells process
Filipin and Nystatin	Caveolae pathway
Liquemin	HSPG pathway
Sodium azide	Endocytic pathways

765

766

767 **Table 2:** Interactions of HPV16 VLPs produced in this study with PMBC (mononuclear

768 cells) from peripheral blood of healthy female volunteers.

PMBC	Receptor	Percentage of cells that interacted with VLPs[1]
Lymphocyte T	CD04	52% ± 3
Lymphocyte T	CD08	47% ± 2
Lymphocyte B	CD20	48% ± 3
Monocyte	CD14	23% ± 5

769

770 [1.] The percentage of cells that interact with HPV16 VLPs was calculated by the number of

771 cells recognized by anti-CD antibodies, which have internalized the particles. The result

772 corresponds to the analysis in duplicate, being representative of at least four trials.

773

774 **Figure 1**

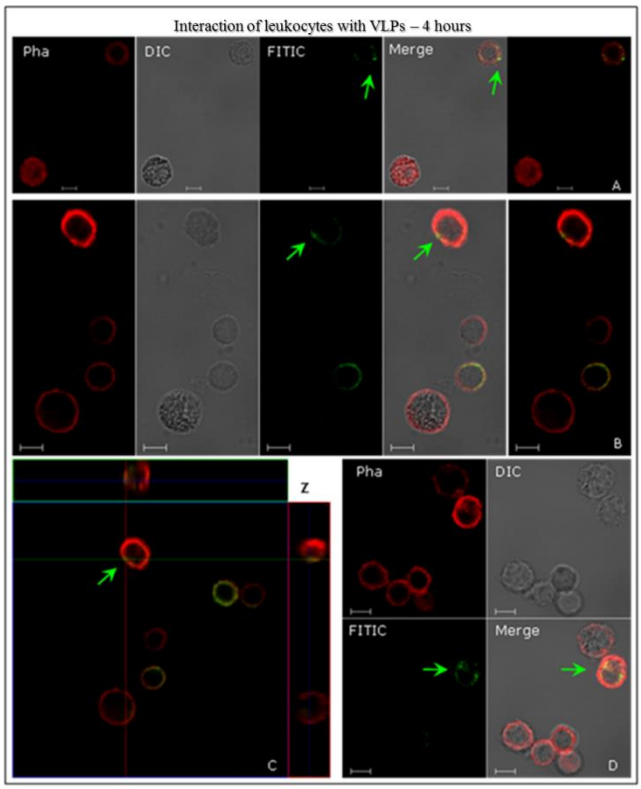

775

776

777 **Figure 2**

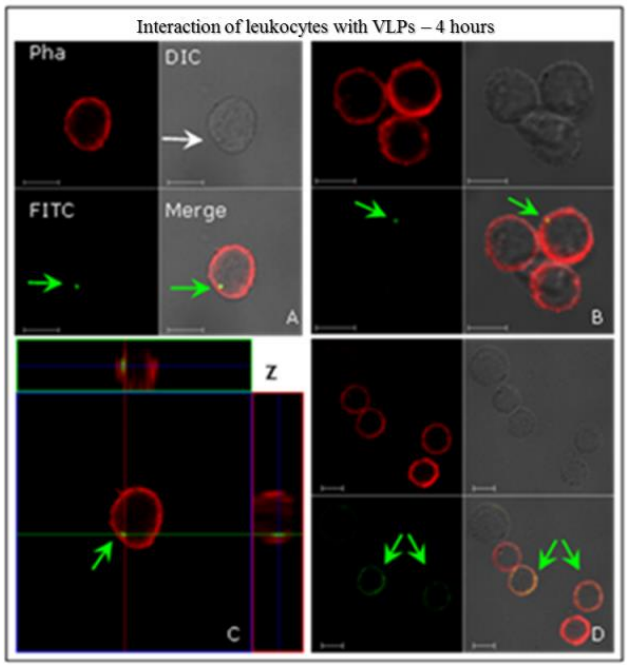

778

779 **Figure 3**

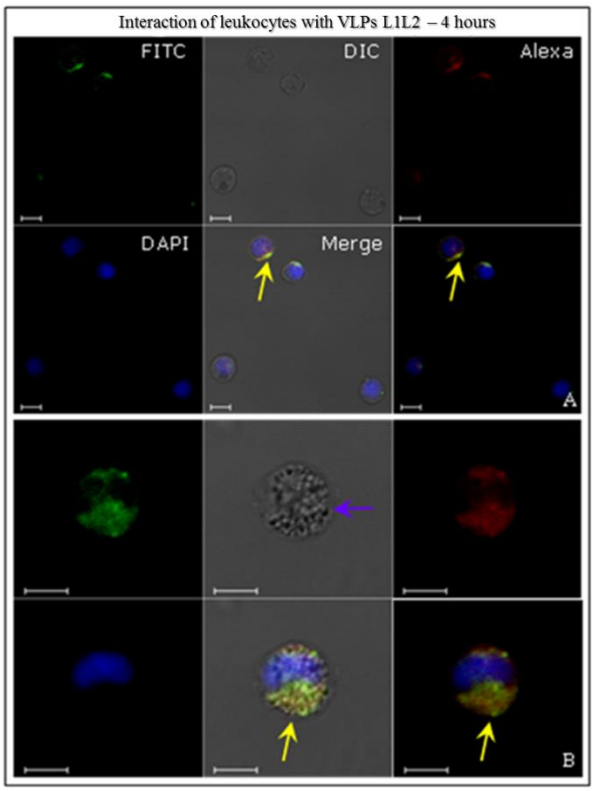

780

781 **Figure 4**

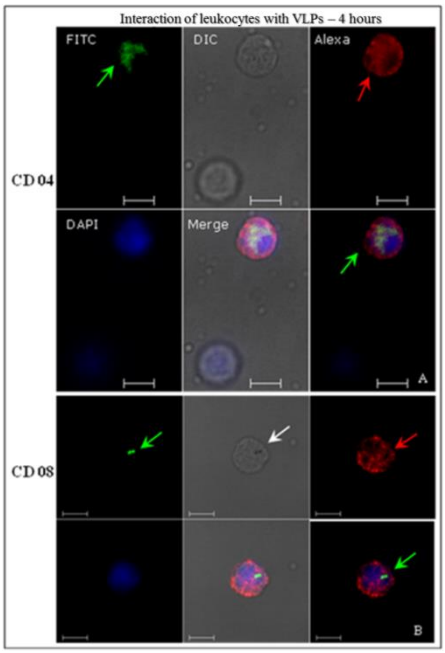

782

783 **Figure 5**

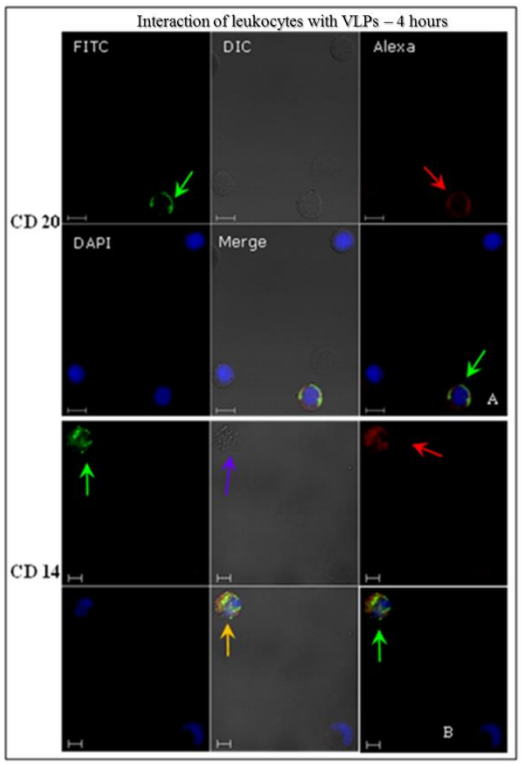

784

785 **Figure 6**

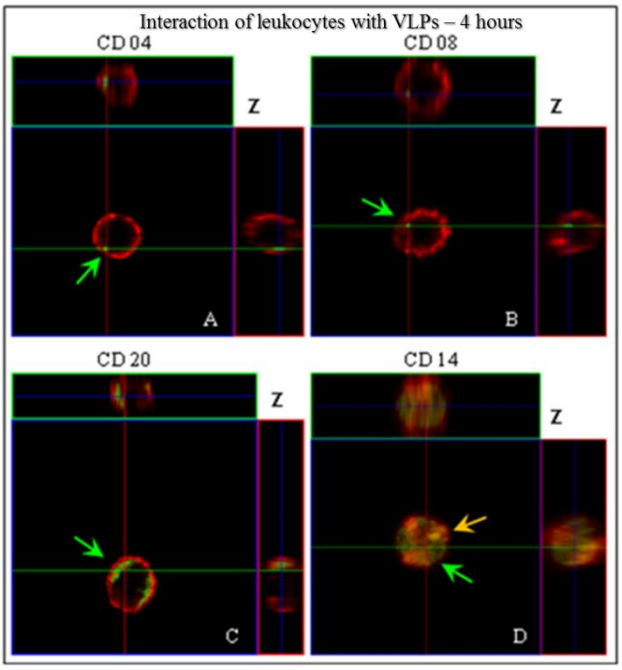

786

787 **Figure 7**

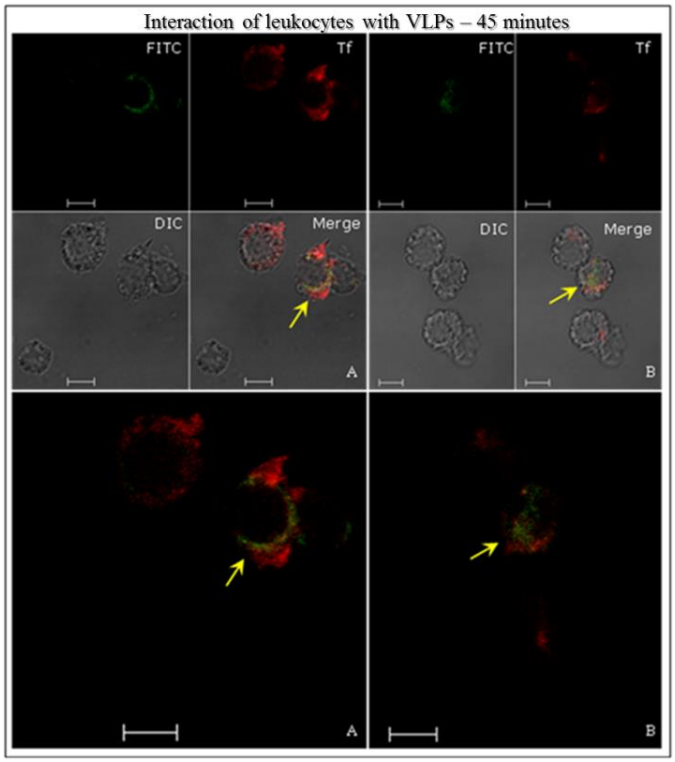

788

789 **Figure 8**

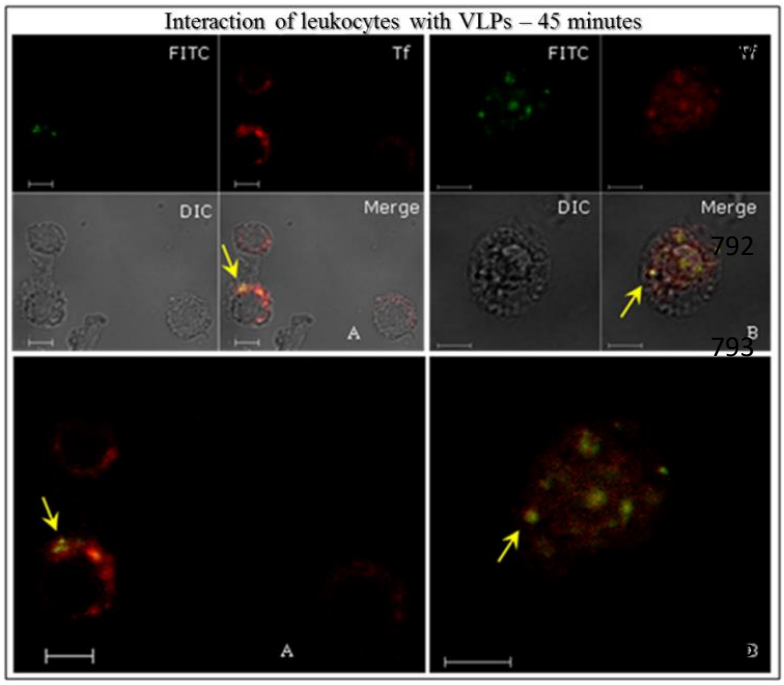

792

793

797 **Figure 9**

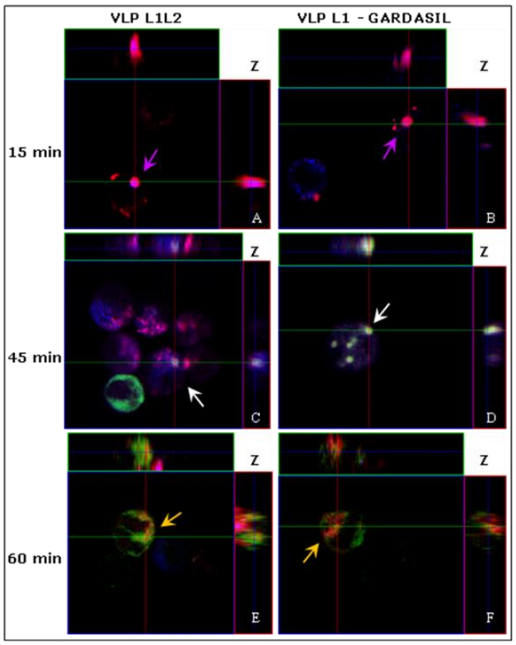

798

799 **Figure 10**

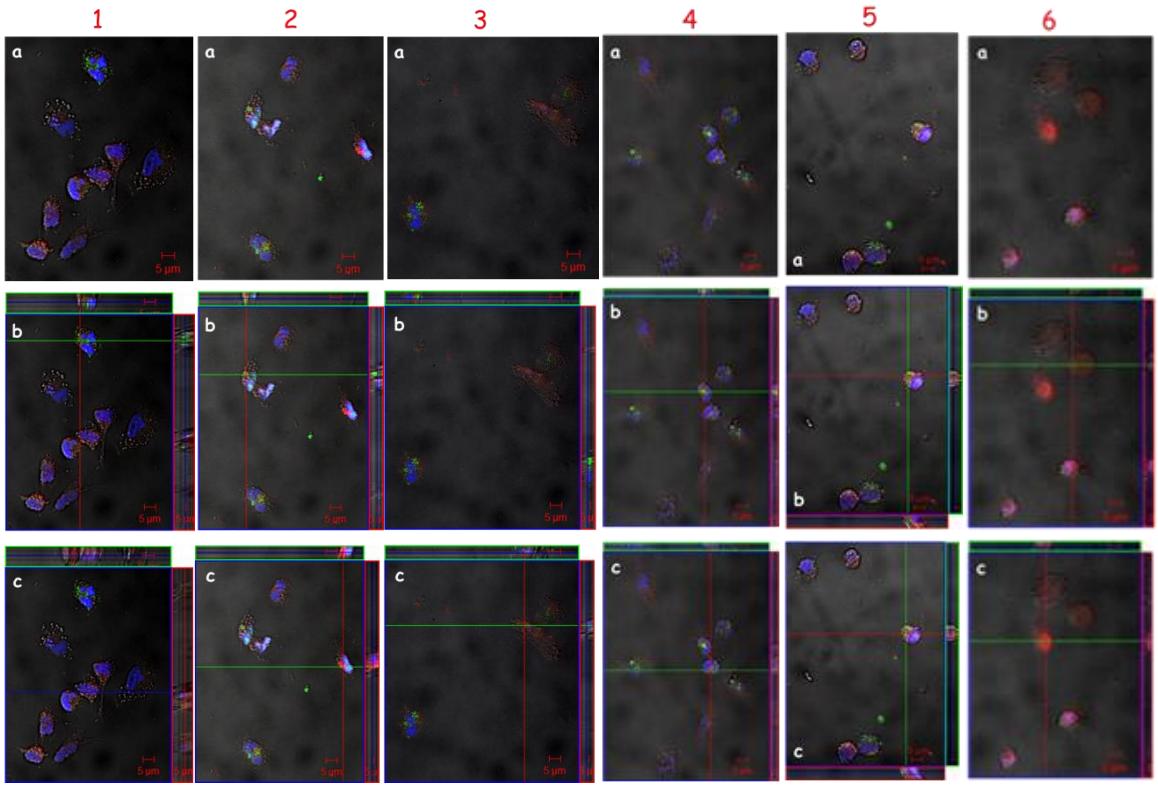

800

801 **Figure 11**

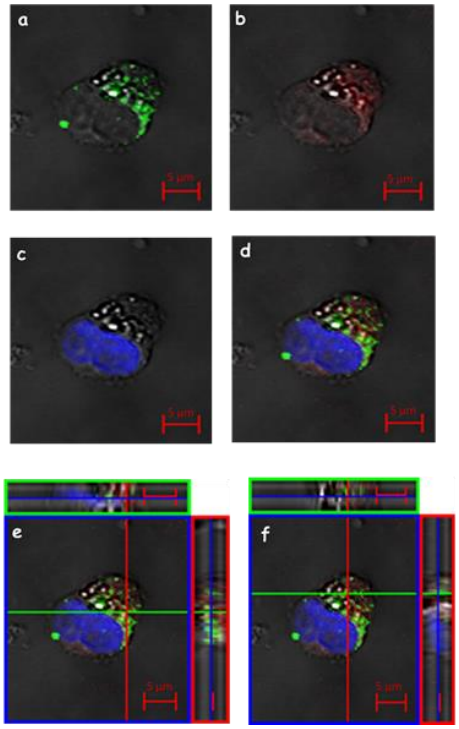

802

803

804

805

806

807

808

809

810

811

812

813

814

815

816

817 **Supplemental Material (Figures S1-S5 and Illustrations S6-S7)**

818 **Image 1 – S1**

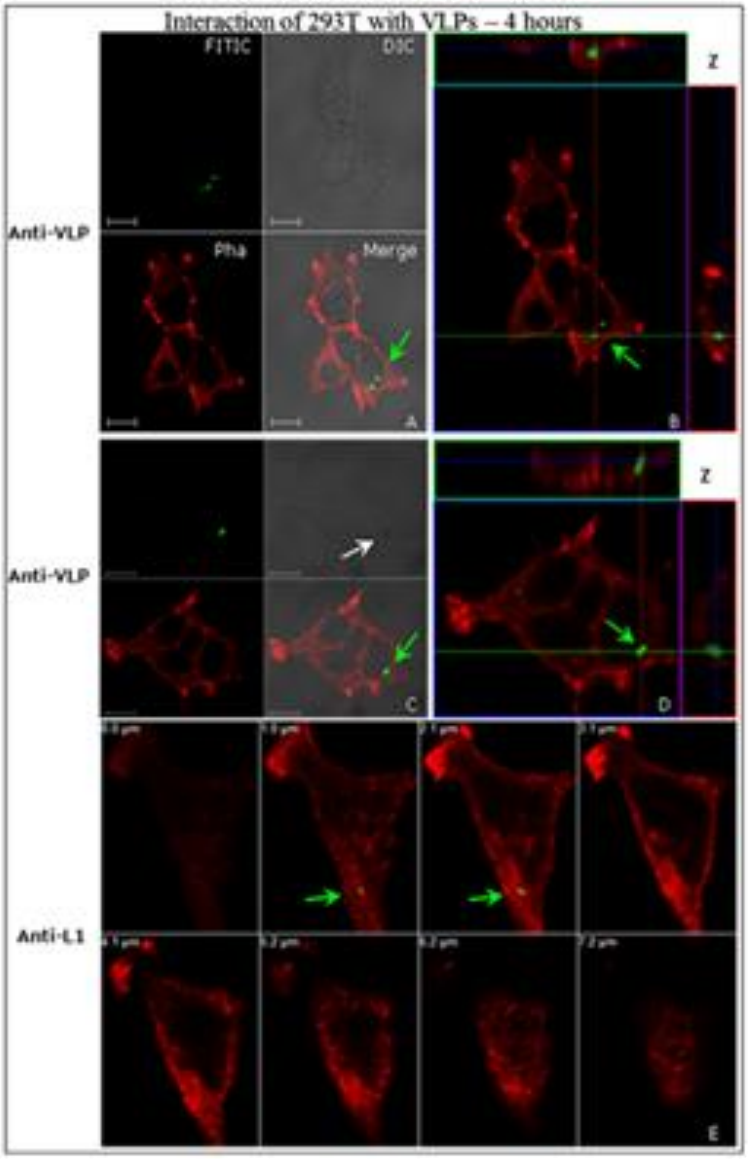

819

820 **Image 1 – S1:** Interaction of non-transfected HEK293T cell line with VLPs of HPV16,

821 detected by indirect immunofluorescence. Cells were incubated with the VLPs for 4 h,

822 fixed with 2% PFA in PBS. In (E) cells were immunostained with anti-L1 antibody and in

823 (A), (B), (C) and (D) anti-VLP conformational antibody, for both HPV16 and developed

824 with secondary antibody conjugated to FITC (green). Phalloidin detected the actin

cytoskeleton with AlexaFluor 594 conjugate (red). The internalisation of VLPs (green arrows) are shown in B and D images, and L1 in E, sweep cuts through the Z axis (B) of 11.38 µm thick sections, and each section with 1.03 µm; (D) 9.67 µm thick sections and each section having 1.61 µm. In (C), there was a similar structure to an endocytic vesicle (white arrow). CLSM Zeiss LSM 510 Meta. Magnification: Objective C-Apochromatic 63xs /1.4 oil. Bar = 10 µm.

Image 2 – S2

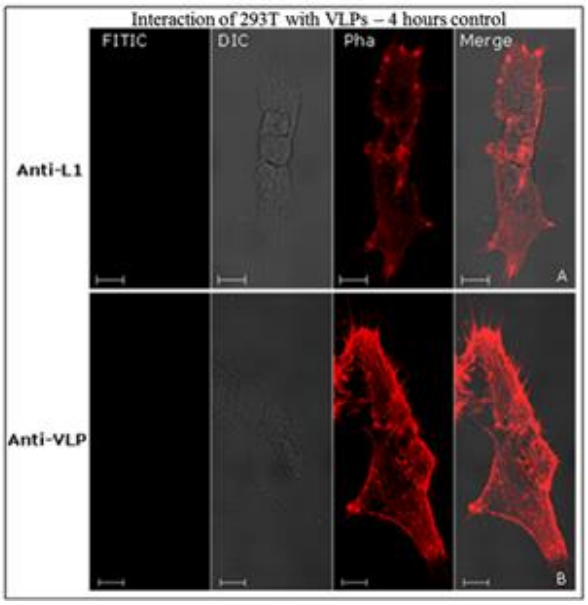

Image 2 S2: Assays-control of the interactions among HEK293T cells non-transfected, with the HPV16 VLPs detected by immunofluorescence. In (A) cells were treated with anti-L1 antibody and (B) with anti-VLP conformational, for both HPV16 and developed with secondary antibody conjugated to FITC (green). AlexaFluor® 594-conjugated Phalloidin (red) detected the actin cytoskeleton. CLSM Zeiss LSM 510 Meta. Magnification: Objective C-Apochromatic 63xs /1.4 oil. Bar =10 µm.

840 **Image 3 – S3**

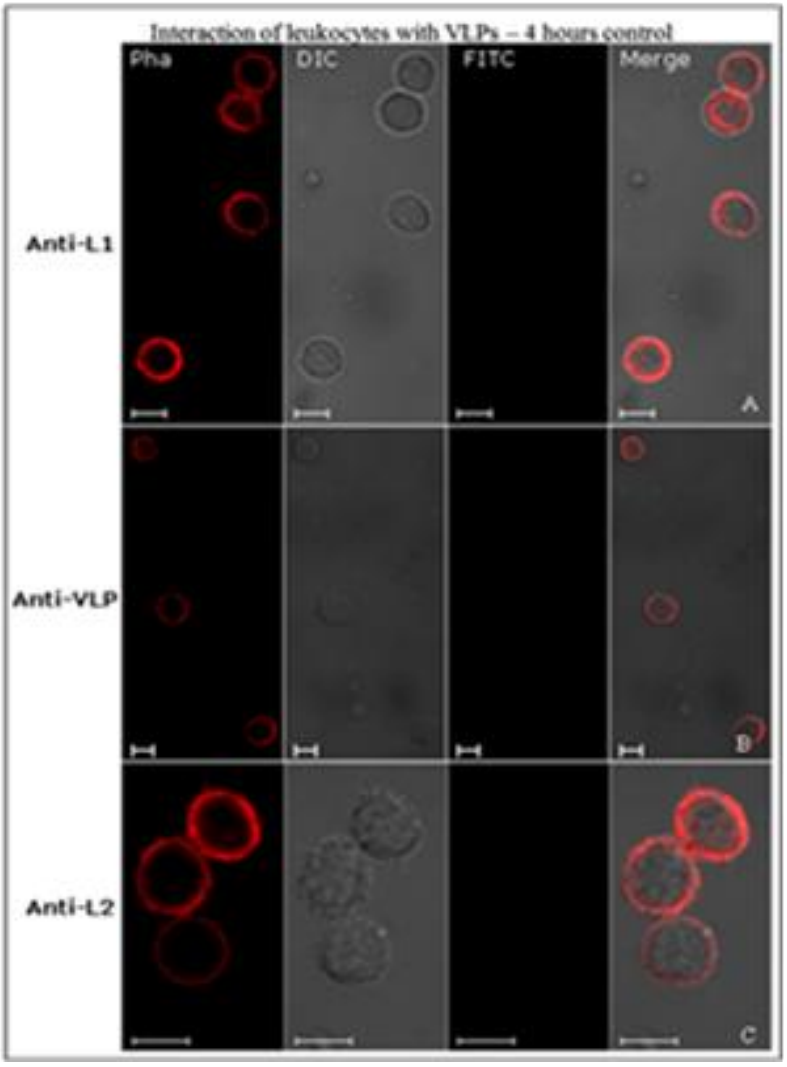

841

842 **Image 3 – S3:** Testing control the interactions of human leukocytes with VLPs of HPV16,
843 detected by indirect immunofluorescence. In (A) the cells were treated with anti-L1 and (B)
844 with anti-VLPs, HPV16 both to, and after, revealed by a secondary antibody conjugated to
845 FITC (green). In (C) the cells were treated with anti-HPV16 L2, and after, AlexaFluor®488
846 revealed by secondary antibody (green). AlexaFluor® 594-conjugated Phalloidin (red)
847 detected the actin cytoskeleton. CLSM Zeiss LSM 510 Meta. Magnification: Objective C-
848 Apochromatic 63xs /1.4 oil. Bar = 5 µm.

849 **Image 4 – S4**

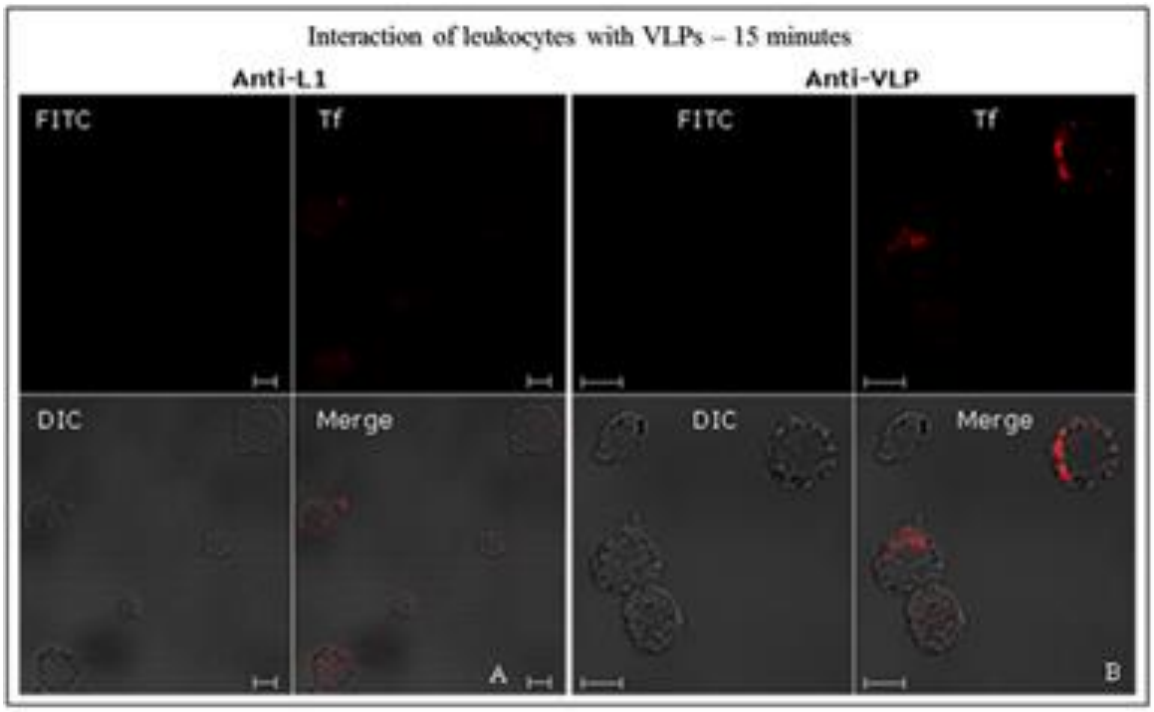

850

851 **Image 4 S4:** Detection of HPV16 VLPs and Tf human leukocytes by indirect
852 immunofluorescence. The leukocyte cells were incubated with the VLPs and Tf protein
853 conjugated TexasRed® (red). In (A) the cells were immunostained with anti-L1 antibody
854 and (B) with anti-VLP conformational both to HPV16, revealed by a secondary antibody
855 conjugated to FITC (green). By confocality (merge) of the images is not possible to observe
856 colocalization and VLPs entry in leukocytes. CLSM Zeiss LSM 510 Meta. Magnification:
857 Objective C-Apochromatic 63xs /1.4 oil. Bar = 5 µm.

858

859

860

861

862

863 **Image 5 – S5**

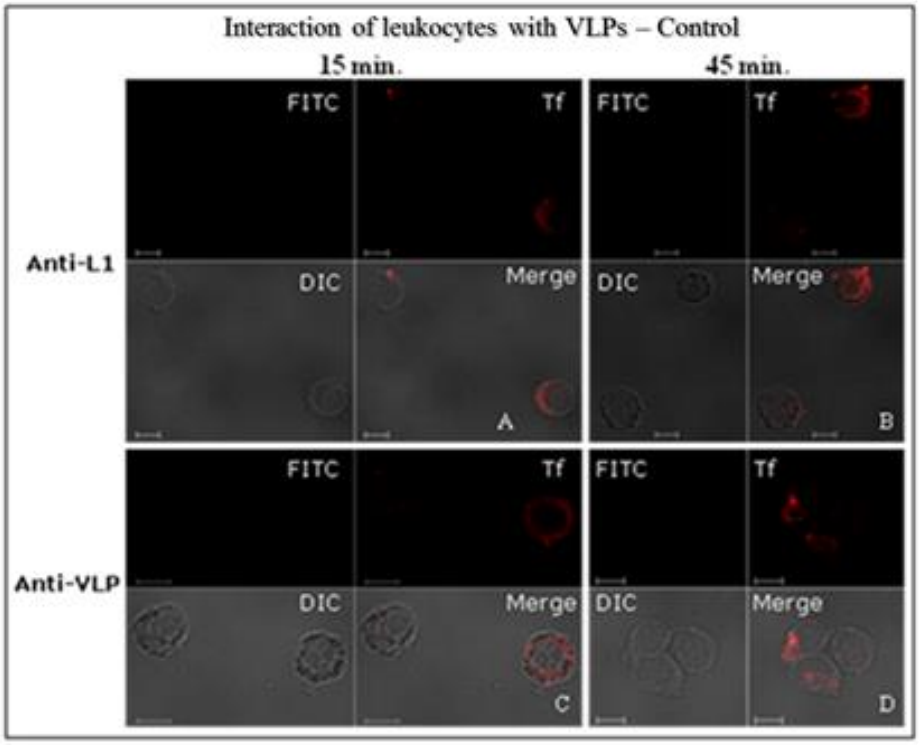

864

865 **Image 5 - S5:** Images of the negative control testing of VLPs of HPV16 and Tf interactions
866 in human leukocytes analysed by indirect immunofluorescence. The leukocyte cells were
867 incubated with Tf conjugated TexasRed® (red) VLPs in the absence (A and C) and / or
868 denatured VLPs (B and D). In (A) and (C) the leukocytes were treated with anti-L1
869 antibody and (B) and (D) anti-VLPs, HPV16 both revealed by a secondary antibody
870 conjugated to FITC (green). Overlay (merge) of images that show no immunostaining signs
871 by anti-L1 and anti-HPV16 VLPs. CLSM Zeiss LSM 510 Meta. Magnification: Objective
872 C-Apochromatic 63xs /1.4 oil. Bar = 5 µm.

873
874
875
876

877 **Illustrations S6 – S7**

878 **S6 - Table 1:** List of primary antibodies used in immunocytochemistry reactions.

Antibody	Dilution	Description	Supplier
Anti-L1 Camvir-1	1:500	anti-mouse IgG_{2a}, specific for HPV16	BD Biosciences
Anti-L1 conformational	1:100	anti-mouse IgG_{2a}, specific for HPV16	Biodesign
Anti-L2	1:100	anti-rabbit IgG	Roden, R. MD/USA
Transferrin conjugated	1:60	TexasRed® (Ex. 595 nm, Em. 615 nm)	Molecular Probes™
Anti-Tf	1:750	anti- rabbit IgG	Dako
Anti-Ferritin	1:750	anti- rabbit IgG	Dako
Anti-CD71	1:750	anti-mouse IgG_1; Tf receptor	Dako
Anti-CD04	1:20	anti-mouse IgG_{2a}; recognizes T lymphocytes "helper"	CALTAG™ Laboratories
Anti-CD08	1:20	anti-mouse IgG_{2a}; recognizes cytotoxic T lymphocytes	CALTAG™ Laboratories
Anti-CD14	1:20	anti-mouse IgG_{2a}; recognizes monocytes	CALTAG™ Laboratories
Anti-CD20	1:20	anti-mouse IgG_3; recognizes B lymphocytes	CALTAG™ Laboratories

879

880 **S7 - Table 2:** List of secondary antibodies used in immunocytochemistry reactions.

Antibody	Dilution	Description	Ex/Em. (nm)	Supplier
FITC	1:250	anti- mouse IgG_{2a}	495/519	BD Biosciences
AlexaFluor®546	1:500	anti- mouse IgG	556/573	Molecular Probes™
AlexaFluor®555	1:500	anti- rabbit IgG	555/565	Molecular Probes™
AlexaFluor®594	1:500	anti- mouse IgG_3	590/617	Molecular Probes™
AlexaFluor®633	1:500	anti- mouse IgG	632/647	Molecular Probes™
AlexaFluor®633	1:500	anti- rabbit IgG	632/647	Molecular Probes™

881